

Article

Press to Success: $\text{Gd}_5\text{FW}_3\text{O}_{16}$ —The First Gadolinium(III) Fluoride Oxidotungstate(VI)

Katharina V. Dorn ^{1,2}  and Ingo Hartenbach ^{1,*}¹ Institute of Inorganic Chemistry, University of Stuttgart, Pfaffenwaldring 55, 70569 Stuttgart, Germany² Department of Materials and Environmental Chemistry, Stockholm University, Svante Arrhenius väg 16 C, 106 91 Stockholm, Sweden

* Correspondence: hartenbach@iac.uni-stuttgart.de; Tel.: +49-711-685-64254

Received: 21 June 2019; Accepted: 12 August 2019; Published: 16 August 2019



Abstract: The gadolinium(III) fluoride oxidotungstate(VI), with the formula $\text{Gd}_5\text{FW}_3\text{O}_{16}$, represents the first published fluoride-derivative of a rare-earth metal oxidotungstate. It is synthesized by a mixture of GdF_3 , Gd_2O_3 , and WO_3 at 800 °C and a pressure of 2 GPa with the help of a belt press. The title compound crystallizes in the monoclinic space group $P2_1/c$ (no. 14) with four formula units per unit cell and the following lattice parameters: $a = 539.29$ (4), $b = 1556.41$ (12), $c = 1522.66$ (11) pm, and $\beta = 93.452$ (4). The crystal structure comprises five crystallographically distinguishable Gd^{3+} cations, which are surrounded by either oxide and fluoride anions (Gd1–3) or by oxide anions only (Gd4, Gd5), with coordination numbers ranging between seven and nine. The fluoride anions are trigonal non-planar coordinated by three Gd^{3+} cations (Gd1–3). The distorted $[\text{WO}_6]^{6-}$ octahedra in this structure form isolates edge- and vertex-connected entities of the compositions $[\text{W}_2\text{O}_{10}]^{8-}$ and $[\text{W}_2\text{O}_{11}]^{10-}$, respectively. According to the presented units, a structured formula can be written as $\text{Gd}_4[\text{FGd}_3]_2[\text{W}_2\text{O}_{10}][\text{W}_2\text{O}_{11}]_2$. The single-crystal Raman spectrum reveals the typical symmetric stretching vibration mode of octahedral oxidotungstate(VI) units at about 871 cm^{-1} .

Keywords: high-pressure; gadolinium; fluorine; tungstate; single-crystal Raman

1. Introduction

Fluoride oxidotungstates (VI), as well as mixed-ligand fluoridooxidotungstates, are known for several alkali, alkaline-earth, and transition metals but not yet for rare-earth elements. Among them, compounds with non-tungsten bonded fluoride, e.g., $\text{Ca}_2\text{NaF}[\text{SiO}_4]$ -type [1] $\text{Na}_3\text{F}[\text{WO}_4]$ [2] are known, while $\text{Li}[\text{W}_3\text{O}_9\text{F}]$ [3], $\text{Na}_5[\text{W}_3\text{O}_9\text{F}_5]$ [4], K_2GeF_6 -type [5], $\text{Cs}_2[\text{WO}_2\text{F}_4]$ [6], $\text{Rb}_2[\text{WO}_2\text{F}_4]$ [7], and $\text{Ag}[\text{WOF}_5]_2$ [8] represent structures, with all F^- anions, of the ligand sphere of hexavalent tungsten both in isolated units or in condensed ones, such as in CuWO_3F_2 [9]. $\text{Ba}_2[\text{WO}_3\text{F}_2]_2$ [10,11] and $\text{Pb}_5\text{W}_3\text{O}_9\text{F}_{10}$ [12] ($\equiv \text{Pb}_{10}[\text{WO}_3\text{F}_3]_4(\text{W}_2\text{O}_6\text{F}_4)\text{F}_4$ with units in parentheses being condensed and those in brackets being isolated) exhibit fluoride anions that are both bonded to W^{6+} and not. Although fluoride-containing rare-earth metal oxido-molybdates with the compositions $\text{REF}[\text{MoO}_4]$ ($\text{RE} = \text{Y}$ [13], $\text{Ce}—\text{Nd}$ [14], $\text{Sm}—\text{Tm}$ [15], and REFMo_2O_7 ($\text{RE} = \text{Y}$ [16], $\text{Eu}—\text{Yb}$ [17]) are well known, the syntheses of the isotopic tungstates is still very challenging. In case of the aforementioned $\text{REF}[\text{MoO}_4]$ representatives, it is possible to utilize molybdenum trioxide both as reactant and as fluxing agent due to its low melting point of 802 °C [18], while in the respective reaction mixture for the tungstates, all components show a melting point above 1200 °C (e.g., GdF_3 : m.p. = 1232 °C; Gd_2O_3 : m.p. = 2425 °C; WO_3 : m.p. = 1473 °C) [18], thus a reaction in silica ampoules would only be possible with another compound as flux. Appropriate candidates, such as alkali metal halides, boron oxide, or molybdenum oxide, all result in undesired side products, such as scheelite-type $\text{ARE}[\text{WO}_4]_2$ representatives (e.g., $\text{NaGd}[\text{WO}_4]_2$ [19]) or rare-earth metal borates and molybdates of various compositions, respectively.

Experiments following a modified solution route with respect to the one of Naruke and Yamase [20] were tried by Schustereit [21] to obtain rare-earth metal fluoride tungstate derivatives; however, no crystalline products were attained. Inspired by single crystals of two $RE(OH)[WO_4]$ derivatives, which occurred during high-pressure experiments to obtain $RE_3Cl_3[WO_6]$ representatives of the smaller rare-earth metals [22,23], the high-pressure synthesis of the formula analogous, and presumably pseudo-isotypic (due to the replacement of OH^- by F^-) $REF[WO_4]$ derivatives, was pursued. Although, the desired products could not be yielded, it was possible to obtain very few single crystals of the gadolinium(III) fluoride oxidotungstate(VI) with the composition $Gd_5FW_3O_{16}$ comprising two different ditungstate units as well as $[FGd_3]^{8+}$ entities — a structural motif known also from $La_3FMO_4O_{16}$ [24] and other fluoride-containing lanthanoid compounds. Hence, the high-pressure synthesis route opens up a possibility to obtain fluoride-containing rare-earth metal(III) oxidotungstates(VI), which may provide suitable host lattices for luminescent cations, e.g., Eu^{3+} and Tb^{3+} , as dopants for compounds of the luminescent innocent rare-earth metals yttrium, lanthanum, gadolinium, and lutetium, analogous to the molybdates, e.g., $YF[MoO_4]:Eu^{3+}$ [13].

2. Materials and Methods

2.1. High-Pressure Synthesis

Single crystals of gadolinium(III) fluoride oxidotungstate(VI), with the formula $Gd_5FW_3O_{16}$ (Figure 1), were received in attempts to synthesize the gadolinium(III) fluoride *ortho*-oxidotungstate(VI) $GdF[WO_4]$ comprising isolated $[WO_4]^{2-}$ tetrahedra. Therefore, the starting materials gadolinium(III) fluoride (GdF_3 : 99.9%, ChemPur, Karlsruhe, Germany), gadolinium sesquioxide (Gd_2O_3 : 99.9%, ChemPur, Karlsruhe, Germany), and tungsten trioxide (WO_3 : 99.9%, Merck, Darmstadt, Germany) were mixed together in a molar ratio of 1:1:3 and finely powdered under argon atmosphere in a glovebox.

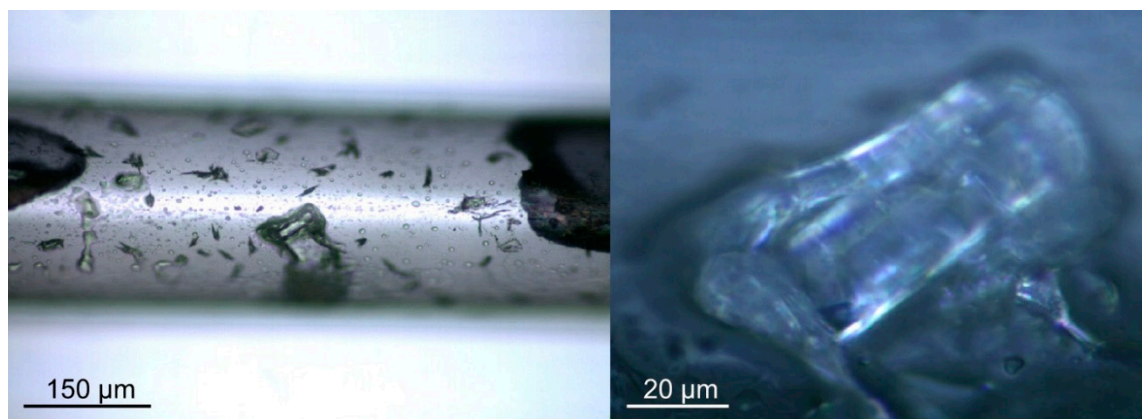


Figure 1. Photos of a single crystal of gadolinium(III) fluoride oxidotungstate(VI) ($Gd_5FW_3O_{16}$) in a glass capillary taken by the optics of a Raman microscope at different magnifications [22].

The mixture was filled into a homemade gold ampoule (purity 99.99%; Figure 2b, top), which was closed with a gold lid and exposed to a reaction temperature of 800 °C and a maximum pressure of 2 GPa for 12 h in a belt press (Figure 2a). Due to the fluoride-containing starting materials and the high-pressure setting, gold was chosen as the most suitable container material. For the title compound $Gd_5FW_3O_{16}$, the following reaction equation assuming a not entirely homogeneous mixture of the starting materials was proposed:



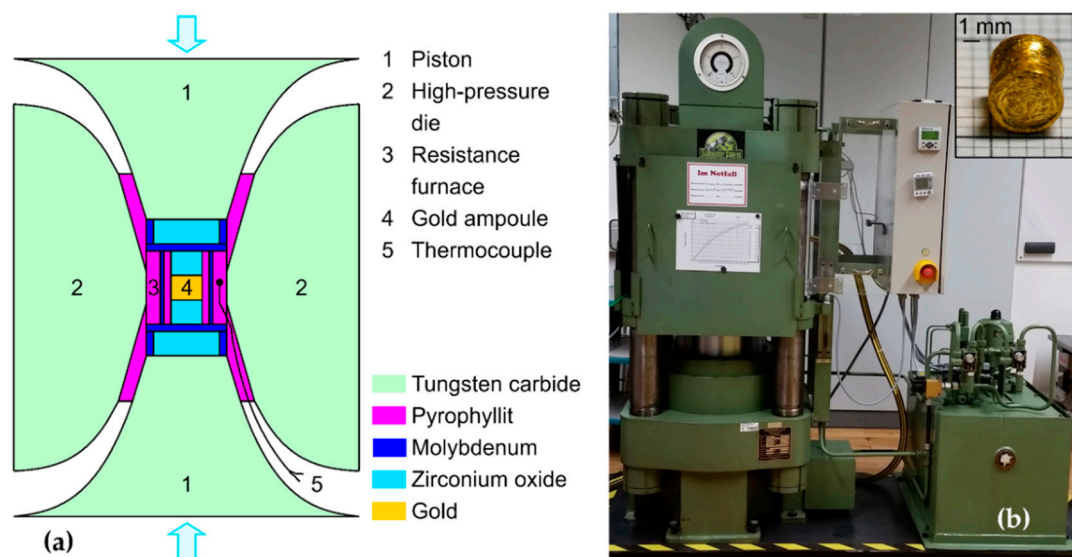


Figure 2. Schematic cross-section (a) of the high-pressure die and the pressure cell of the belt press at the Max-Planck-Institute for Solid State Research (Stuttgart, Germany), and the gold ampoule after treatment ((b), top).

Due to the extremely small amount of reaction mixture (approx. 50 mg) within the gold ampoules, only very few single crystals of the title compound were obtained. The identification of expected by-products, such as GdOF or $\text{GdF}[\text{WO}_4]$, was not possible.

2.2. Single-Crystal Structure Determination

Intensity data sets for the title compound $\text{Gd}_5\text{FW}_3\text{O}_{16}$ were collected with a Smart Apex II Duo single-crystal diffractometer (Bruker AXS, Karlsruhe, Germany) by using Mo-K_α radiation ($\lambda = 71.07$ pm) at a temperature of $T = 130(2)$ K. Data correction was applied by the program SADABS [25], and crystal structure solution and refinement were performed with the program package SHELX-2013 [26]. The crystallographic data are displayed in Table 1, while atomic positions and coefficients of the isotropic thermal displacement parameters are given in Table 2. Due to the high absorption of both gadolinium and tungsten, it was not possible to refine all oxygen atoms anisotropically; hence only isotropic refinements for all 16 crystallographically independent O^{2-} anions were performed. The rather high residual electron density, mainly around $(\text{Gd}5)^{3+}$, results from the quite peculiar surrounding of this cation (see Section 3.1). Attempts to solve the structure with the aforementioned cation at a split position (also to resolve the pronouncedly prolate displacement ellipsoid) were not successful. Furthermore, a variation in the occupation of the $(\text{Gd}5)$ site, such as defect, mixed, or single occupation with Au^{3+} (from the container material), resulted in either a full occupation with gadolinium after refinement or in significantly worse residual values (for the occupation of the aforementioned site with gold).

Table 1. Crystallographic data for gadolinium (III) fluoride oxidotungstate (VI) (Gd₅FW₃O₁₆).

Crystal System	Monoclinic
Space group	<i>P</i> 2 ₁ / <i>c</i> (no. 14)
Formula units, <i>Z</i>	4
<i>a</i> /pm	539.29(4)
<i>b</i> /pm	1556.41(12)
<i>c</i> /pm	1522.66(11)
β /°	93.452(4)
Density, <i>D_x</i> /g·cm ^{−3}	8.397
Molar volume, <i>V</i> /cm ³ ·mol ^{−1}	192.07
Single-crystal X-ray diffractometer	Smart Apex II Duo (Bruker AXS)
Radiation	71.07 (Mo- <i>K</i> _α)
Temperature, <i>T</i> /K	130(2)
Data corrections	Program SADABS [25]
Structure solution and refinement	Program package SHELX-2013 [26], scattering factors according to [27]
Index range, $\pm h/\pm k/\pm l$	8/23/23
$2\theta_{max}$ /°	66.40
<i>F</i> (000)	2716
Absorption coefficient, μ	52.64
Reflections collected/unique	22613/4758
Refined parameters	147
<i>R</i> _{int} / <i>R</i> _σ	0.058/0.059
<i>R</i> ₁ for (<i>n</i>) reflections with $ F_o \geq 4\sigma(F_o)$	0.033 (3728)
<i>R</i> ₁ / <i>wR</i> ₂ for all reflections	0.052/0.047
Goodness of Fit, <i>S</i>	1.005
Extinction, <i>g</i>	0.00078 (1)
Residual electron density, $\rho_{min/max}$ /e [−] 10 ^{−6} pm ^{−3}	−4.98/3.95 at (Gd5) ³⁺

Table 2. Wyckoff positions, fractional atomic coordinates, and equivalent isotropic displacement parameters (*U*_{eq}¹) for Gd₅FW₃O₁₆.

Atom	Position	<i>x</i> / <i>a</i>	<i>y</i> / <i>b</i>	<i>z</i> / <i>c</i>	<i>U</i> _{eq} /pm ²
Gd1	4e	0.54505(6)	0.22505(2)	0.86095(2)	51.2(8)
Gd2	4e	0.99526(6)	0.15440(2)	0.22655(2)	47.8(7)
Gd3	4e	0.02811(6)	0.11780(2)	0.47811(2)	48.0(8)
Gd4	4e	0.48355(6)	0.02332(2)	0.12010(2)	43.4(8)
Gd5	4e	0.98901(8)	0.09537(3)	0.72614(3)	152.9(10)
F	4e	0.1920(7)	0.1929(3)	0.3634(3)	67(9)
W1	4e	0.00855(5)	0.10733(2)	0.97043(2)	41.7(7)
W2	4e	0.54455(5)	0.21721(2)	0.63497(2)	42.4(6)
W3	4e	0.56511(5)	0.02705(2)	0.34505(2)	42.7(6)
O1	4e	0.8804(8)	0.2125(3)	0.9665(3)	58(10)
O2	4e	0.1430(9)	0.1177(3)	0.0836(3)	67(10)
O3	4e	0.2830(9)	0.1171(3)	0.9023(3)	67(11)
O4	4e	0.7770(8)	0.0232(3)	0.0125(3)	48(10)
O5	4e	0.8007(8)	0.0847(3)	0.8614(3)	50(10)
O6	4e	0.3607(9)	0.2020(3)	0.5350(3)	80(11)
O7	4e	0.6309(9)	0.1708(3)	0.1260(3)	57(10)
O8	4e	0.8288(9)	0.1619(3)	0.5964(3)	75(11)
O9	4e	0.2937(9)	0.2284(3)	0.7170(3)	85(11)
O10	4e	0.7822(8)	0.2219(3)	0.7491(3)	46(10)
O11	4e	0.5031(9)	0.0898(3)	0.6852(3)	98(11)
O12	4e	0.3689(9)	0.0384(3)	0.4321(3)	80(10)
O13	4e	0.3196(9)	0.0591(3)	0.2558(3)	101(11)
O14	4e	0.7181(9)	0.1391(3)	0.3603(3)	83(11)
O15	4e	0.1307(9)	0.0152(3)	0.5929(3)	64(10)
O16	4e	0.7875(8)	0.0239(3)	0.2326(3)	51(10)

$$^1 U_{eq} = \frac{1}{3} \left[U_{22} + \frac{1}{\sin^2(\beta)} (U_{11} + U_{33} - 2U_{13} \cos(\beta)) \right] [28].$$

2.3. Single-Crystal Raman Spectroscopy

The single-crystal Raman spectrum for the title compound $Gd_5FW_3O_{16}$ was measured with the help of a Horiba XploRa spectrometer using a LASER device of the wavelength $\lambda = 532$ nm. For this purpose, the crystal was placed in a glass capillary and fixed with desiccator grease (Figure 1).

3. Results and Discussion

3.1. Crystal Structure

The first gadolinium(III) fluoride oxidotungstate(VI), with the empirical formula $Gd_5FW_3O_{16}$, crystallizes in the monoclinic space group $P2_1/c$ (no. 14) with four formula units per unit cell and the lattice parameters $a = 539.29(4)$, $b = 1556.41(12)$, $c = 1522.66(11)$ pm, and $\beta = 93.452(4)$ (Table 1). The motifs of mutual adjunction [29–31], as well as selected interatomic distances (d /pm) and bond angles (\angle°), in the crystal structure of $Gd_5FW_3O_{16}$, are summarized in Tables 3–5.

Table 3. Selected interatomic distances (d /pm) in the crystal structure of $Gd_5FW_3O_{16}$.

Distance		Distance		Distance		Distance	
Gd1–F	229.4(4)	Gd2–F	235.8(4)	Gd3–F	232.1(4)	Gd4–O2	239.1(5)
Gd1–O1	235.4(5)	Gd2–O2	243.0(5)	Gd3–O1	276.1(5)	Gd4–O3	255.5(5)
Gd1–O3	230.8(5)	Gd2–O7	243.1(5)	Gd3–O6	234.4(5)	Gd4–O4	234.5(5)
Gd1–O5	258.3(5)	Gd2–O9	244.3(5)	Gd3–O8	225.9(5)	Gd4–O4'	249.7(5)
Gd1–O9	250.8(5)	Gd2–O10	227.9(5)	Gd3–O12	235.6(5)	Gd4–O5	230.3(5)
Gd1–O10	219.0(5)	Gd2–O13	231.6(5)	Gd3–O14	240.0(5)	Gd4–O7	242.9(5)
Gd1–O14	231.2(5)	Gd2–O14	260.9(5)	Gd3–O15	240.8(5)	Gd4–O13	236.6(5)
		Gd2–O16	232.4(5)	Gd3–O15'	246.5(5)	Gd4–O16	229.8(5)
Gd5–O5	235.7(5)	W1–O1	177.6(5)	W2–O6	178.2(5)	W3–O11	190.6(5)
Gd5–O8	234.8(5)	W1–O2	183.6(5)	W2–O7	181.1(5)	W3–O12	175.4(5)
Gd5–O9	265.2(5)	W1–O3	186.4(5)	W2–O8	188.3(5)	W3–O13	190.5(5)
Gd5–O10	230.0(5)	W1–O4	194.5(5)	W2–O9	190.4(5)	W3–O14	193.7(5)
Gd5–O11	265.8(5)	W1–O4'	234.4(5)	W2–O10	209.8(5)	W3–O15	195.7(5)
Gd5–O11'	287.9(5)	W1–O5	197.8(5)	W2–O11	214.3(5)	W3–O16	215.0(5)
Gd5–O13	294.6(5)						
Gd5–O15	253.9(5)						
Gd5–O16	228.1(5)						

Table 4. Selected bond angles (\angle°) in the crystal structure of $Gd_5FW_3O_{16}$.

Angle	
Gd1–F–Gd2	(1x) 117.2(2)
Gd1–F–Gd3	(1x) 130.3(2)
Gd2–F–Gd3	(1x) 111.4(2)
W1–O4–W1	(2x) 107.3(2)
O4–W1–O4'	(2x) 72.7(2)
W2–O11–W3	(1x) 145.0(3)

Table 5. Motifs of mutual adjunction [29–31] and effective coordination numbers (ECoN) [32] for the cations in the crystal structure of Gd₅FW₃O₁₆.

Atom	Gd1	Gd2	Gd3	Gd4	Gd5	W1	W2	W3	C.N.
F	1/1	1/1	1/1	0/0	0/0	0/0	0/0	0/0	3
O1	1/1	0/0	1/1	0/0	0/0	1/1	0/0	0/0	3
O2	0/0	1/1	0/0	1/1	0/0	1/1	0/0	0/0	3
O3	1/1	0/0	0/0	1/1	0/0	1/1	0/0	0/0	3
O4	0/0	0/0	0/0	2/2	0/0	2/2	0/0	0/0	4
O5	1/1	0/0	0/0	1/1	1/1	1/1	0/0	0/0	4
O6	0/0	0/0	1/1	0/0	0/0	0/0	1/1	0/0	2
O7	0/0	1/1	0/0	1/1	0/0	0/0	1/1	0/0	3
O8	0/0	0/0	1/1	0/0	1/1	0/0	1/1	0/0	3
O9	1/1	1/1	0/0	0/0	1/1	0/0	1/1	0/0	4
O10	1/1	1/1	0/0	0/0	1/1	0/0	1/1	0/0	4
O11	0/0	0/0	0/0	0/0	2/2	0/0	1/1	1/1	4
O12	0/0	0/0	1/1	0/0	0/0	0/0	0/0	1/1	2
O13	0/0	1/1	0/0	1/1	1/1	0/0	0/0	1/1	4
O14	1/1	1/1	1/1	0/0	0/0	0/0	0/0	1/1	4
O15	0/0	0/0	2/2	0/0	1/1	0/0	0/0	1/1	4
O16	0/0	1/1	0/0	1/1	1/1	0/0	0/0	1/1	4
C.N.	7	8	8	8	9	6	6	6	
ECoN	6.2	7.4	7.2	7.6	6.3	4.8	4.8	5.0	

The crystal structure of Gd₅FW₃O₁₆ comprises five crystallographically distinguishable Gd³⁺ cations (Tables 2 and 3) with coordination numbers of seven (Gd1), eight (Gd2–Gd4), and nine (Gd5) set up by both oxide and fluoride anions (Gd1–Gd3) and only by oxide anions (Gd4, Gd5), respectively. While the coordination polyhedra of the cations (Gd1)³⁺, (Gd3)³⁺, and (Gd5)³⁺ are irregularly shaped, the ones for (Gd2)³⁺ and (Gd4)³⁺ can be described as distorted square antiprisms (Figure 3). Both the Gd³⁺–O^{2−} distances of 219–295 pm and the Gd³⁺–F[−] distances of 230–236 pm (Table 3) are in good accordance to correspondent values found in literature (e.g., in Gd₄O₃F₆ (C.N. (Gd³⁺) = 9 + 4): $d(\text{Gd}^{3+}\text{--O}^{2-}) = 215\text{--}296$ pm, $d(\text{Gd}^{3+}\text{--F}^-) = 215\text{--}278$ pm [33]). The fluoride anions are surrounded by three Gd³⁺ cations (Gd1–Gd3) with a deviation of about 14 pm out of the plane built up by the F[−] anions (Figure 3, bottom right) and Gd–F–Gd bond angles of 111–130° (Table 4). A very similar environment of the fluoride anions is found in the crystal structure of the lanthanum(III) fluoride oxidomolybdate(VI) of the composition La₃FMo₄O₁₆ [24], in which the La–F–La bond angles range between 108 and 137° and the deviation of the fluoride atoms out of the plane built up by La³⁺ cations is about 24 pm. For (Gd5)³⁺, a rather high and very prolate displacement ellipsoid is noticeable (see Figure 3 bottom left), which can be explained by an anisotropic distribution of the distances between these cations and their surrounding oxide ligands. Although being the gadolinium cation with the highest coordination number, only four O^{2−} anions (O5, O8, O10, O16) are found with distances shorter than 236 pm. These form a belt (or very flat tetrahedron) around (Gd5)³⁺, roughly situated in the crystallographic (241) layer. Hence, these cations “escape” the stress of a tight, almost two-dimensional surrounding by extending their displacement anisotropically perpendicular to the aforementioned layer. Of the five oxygen atoms with distances longer than 250 pm, the shortest one (O15) also resides within the aforementioned belt, while the four longest ones (O9, O11, O11′, O13) are situated in the direction of the longest principal axis of the displacement ellipsoid of (Gd5)³⁺.

These findings are also corroborated by both MAPLE [29–31] and bond valence calculations [34,35]. The effective coordination numbers (ECoN, [33]) of Gd1–4 are at best about 0.8 less than the real ones (Table 5), whereas (Gd5)³⁺ exhibits an ECoN value of 6.3, which is only 70% of the nine surrounding oxide anions detected from the crystal structure description, due to this anisotropic distance distribution. The contribution of every single oxygen ligand to the effective coordination number displays a gap from the ideal value of 1 ± 0.2 for the four shortest ones to 0.63 for (O5)^{2−} and between 0.4 and 0.08

for the longest contacts. The same is true for the bond valence calculations, in which Gd1–4 result to an average charge of 3.1, while it amounts for Gd5 to less than 2.9, with the O^{2-} atoms showing the shortest contacts delivering between 0.5 and 0.4 to the overall charge (0.27 for O15 with the median bond length), and the other five provide 0.2 and less (bond-valence parameters for $Gd^{3+}-O^{2-}$ contacts: $R_0 = 2.065 \text{ \AA}$, $B = 0.37$ [35]). Thus, the coordination number around the $(Gd5)^{3+}$ cations is better described as five *plus four* instead of nine.

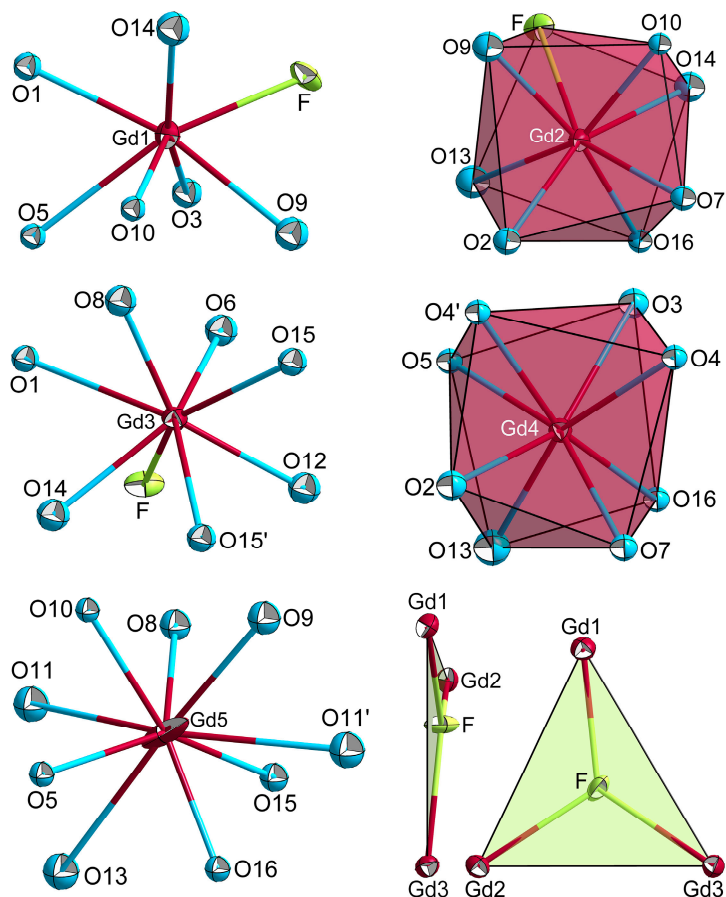


Figure 3. Coordination environments of the five crystallographically distinguishable Gd^{3+} cations (red) and trigonal non-planar coordination polyhedra of the fluoride anions (green) in the crystal structure of $Gd_5FW_3O_{16}$ (ellipsoid representation at 95% probability).

The crystal structure of $Gd_5FW_3O_{16}$ further comprises three crystallographically distinguishable W^{6+} cations, which are surrounded by six oxide anions each in shape of distorted octahedra (Figure 4). These coordination polyhedra are interconnected via edge- and vertex-sharing to discrete $[(W1)_2O_{10}]^{8-}$ and $[(W2)(W3)O_{11}]^{10-}$ entities, respectively (Figure 4). The $W^{6+}-O^{2-}$ distances range from 175 (terminal) to 234 pm (connecting) with the values in between, resembling the overall coordination of the oxygen anion, i.e., the less contact to Gd^{3+} cations, the shorter the $W^{6+}-O^{2-}$ bond length (Table 4). These values are typical for octahedral oxidotungstates(VI), especially those in Keggin polyhedra comprising both, terminal as well as edge and vertex sharing oxygen atoms (e.g. $H_3PW_{12}O_{40}$: $d(W^{6+}-O^{2-}) = 169\text{--}245 \text{ pm}$ [36]). While the interaction between the oxide anions and the gadolinium cations is of a mainly ionic nature, the bond between oxygen and tungsten can better be described as covalent. Thus, the anionic arrangement is determined by the previously described isolated ditungstate entities, and the Gd^{3+} cations are arranged in suitable voids (together with the F^- anions). However, the voids filled by the $(Gd5)^{3+}$ cations appear not to be as suitable as those for $(Gd1\text{--}4)^{3+}$; hence the anisotropic distance distribution found for the coordination polyhedra around the $(Gd5)^{3+}$ cations is explainable.

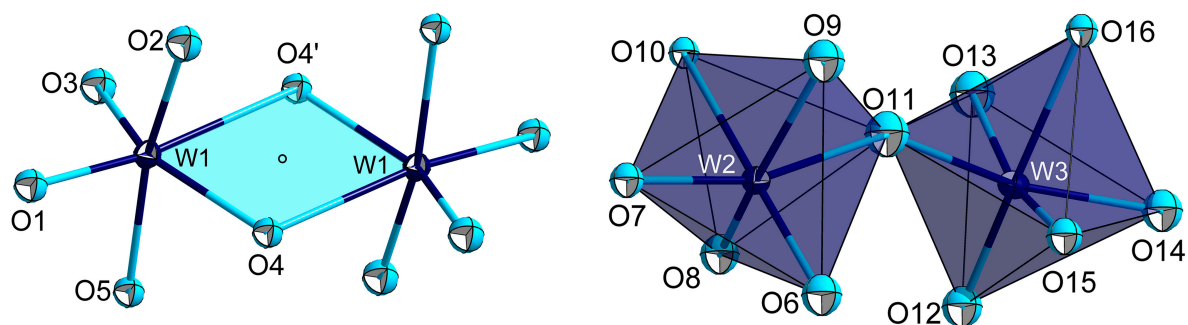


Figure 4. Distorted $[\text{WO}_6]^{6-}$ octahedra in the crystal structure of $\text{Gd}_5\text{FW}_3\text{O}_{16}$ (ellipsoid representation at 95% probability), which are connected via common edges to discrete $[(\text{W}1)_2\text{O}_{10}]^{8-}$ units comprising an inversion center \circ (left) and by sharing vertices to also discrete $[(\text{W}2)(\text{W}3)\text{O}_{11}]^{10-}$ entities (right).

A view at the expanded unit cell of $\text{Gd}_5\text{FW}_3\text{O}_{16}$ is given in Figure 5. Based on the previously mentioned building blocks, namely the two molecular ditungstate units $[\text{W}_2\text{O}_{10}]^{8-}$ and $[\text{W}_2\text{O}_{11}]^{10-}$, the anionic but non-covalent $[\text{FGd}_3]^{8+}$ triangles, and the remaining two Gd^{3+} cations, Gd4 and Gd5, this first gadolinium fluoride oxidotungstate (VI) can be described with a structured formula according to $\text{Gd}_4[\text{FGd}_3]_2[\text{W}_2\text{O}_{10}][\text{W}_2\text{O}_{11}]_2$.

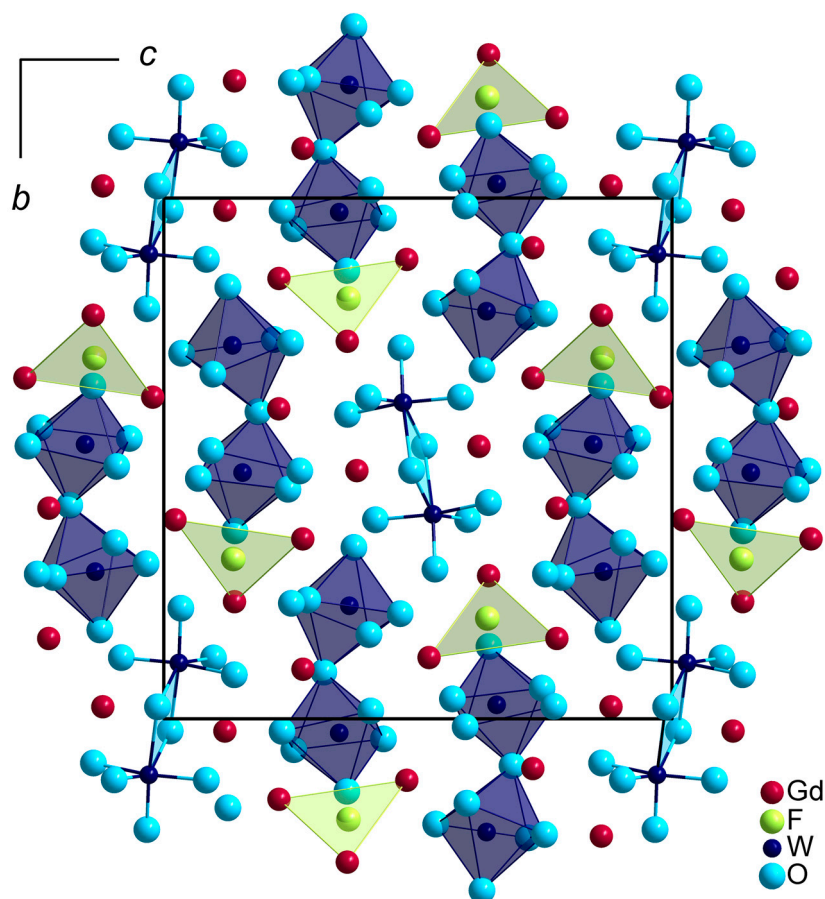


Figure 5. View at the expanded unit cell of $\text{Gd}_5\text{FW}_3\text{O}_{16}$ along $[100]$ emphasizing $[(\text{O}4)_2(\text{W}1)_2]^{8+}$ rhombuses of the $[(\text{W}1)_2\text{O}_{10}]^{8-}$ entities (light blue), $[(\text{W}2)(\text{W}3)\text{O}_{11}]^{10-}$ units (dark blue), and the trigonal non-planar coordination environments of the F^- anions (green).

3.2. Single-Crystal Raman Spectrum

The single-crystal Raman spectrum (Figure 6) shows the band of the symmetric vibration mode of the distorted octahedral $[\text{WO}_6]^{6-}$ entities in the crystal structure of $\text{Gd}_5\text{FW}_3\text{O}_{16}$ at a Raman shift of 871 cm^{-1} . This shift is in good accordance with data from both, compounds consisting of vertex-sharing octahedra like russelite (Bi_2WO_6) [37] and minerals comprising edge-connected octahedral units, such as hübnerite (MnWO_4) [37], ferberite (FeWO_4) [37], and raspite ($\alpha\text{-PbWO}_4$) [37], with their symmetric vibration modes ranging between 800 and 885 cm^{-1} . Due to the large background caused by the desiccator grease (also responsible for the modes between 1000 and 1500 cm^{-1} , as well as between 2600 and 3100 cm^{-1} [38,39]) in combination with the very small single crystal (Figure 1), the less intense antisymmetric stretching, as well as the deformation vibrations, can only be adumbrated in the area below 850 cm^{-1} (inset of Figure 6). Other than preliminary experiments using a belt press, in which a contamination with H_2O lead to hydroxide containing products, the absence of OH groups in the presented compound is proved by the missing vibration mode at about 3500 cm^{-1} [40,41], which is a crucial point for the corroboration of the overall composition since F^- and OH^- groups behave isosteric and the single crystals have proven to be too small for a reliable microprobe analysis.

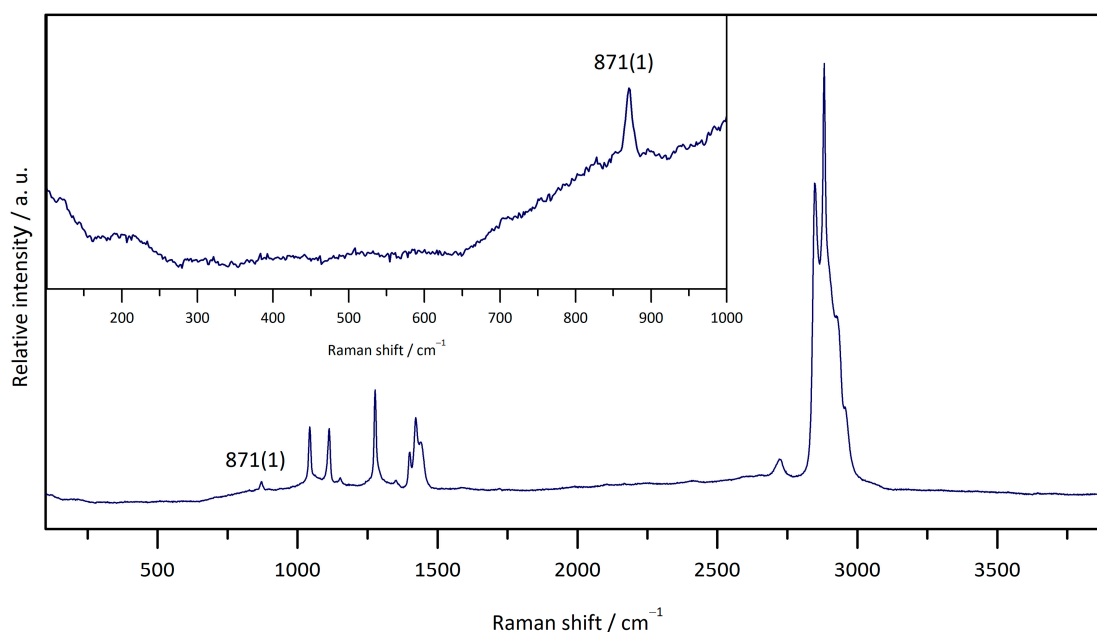


Figure 6. Single-crystal Raman spectrum of $\text{Gd}_5\text{FW}_3\text{O}_{16}$ (only visible band at 871 cm^{-1}) embedded in desiccator grease (bands between 1000 and 3100 cm^{-1}) under excitation with a green LASER ($\lambda = 532\text{ nm}$).

4. Conclusions

The new gadolinium (III) fluoride oxidotungstate (VI), $\text{Gd}_5\text{FW}_3\text{O}_{16}$ ($\cong \text{Gd}_4[\text{FGd}_3]_2[\text{W}_2\text{O}_{10}][\text{W}_2\text{O}_{11}]_2$), was synthesized via high-pressure methods in gold ampoules using a belt press and GdF_3 , Gd_2O_3 , and WO_3 as starting materials. The characterization was carried out in single-crystal diffraction and Raman spectroscopy. This fluoride derivative of a rare-earth metal oxidotungstate marks the first success in the syntheses of this class of compounds, while numerous synthesis attempts with both solid-state and solvochemical methods failed to yield crystalline products. Although the high-pressure synthesis has proven to be successful, a high yield of the product could not be established due to the small sample size. However, since elevated pressure appears to have a positive effect on the formation of rare-earth metal fluoride tungstates, there is a good chance to produce a larger amount with hydrothermal methods. Appropriate experiments are already underway, and if a single-phase

synthesis has proven to be successful, these materials are rather promising for doping with active cations for luminescence purposes.

Author Contributions: Conceptualization, K.V.D. and I.H.; investigation, K.V.D.; resources, I.H.; writing—original draft preparation, K.V.D.; writing—review and editing, I.H.; supervision, I.H.

Acknowledgments: We are indebted to Adrian Geyer for measuring the single-crystal Raman spectrum with the Raman microscope of Hans-Joachim Massonne (Institute of Mineralogy and Crystal Chemistry, University of Stuttgart, Germany), and Graham McNally, Frank Falkenberg, and Hidenori Takagi for the opportunity to use the belt press at the Max-Planck-Institute for Solid-State Research (Stuttgart, Germany). Furthermore, we thank Wolfgang Frey (Institute for Organic Chemistry, University of Stuttgart, Germany) for the collection of the single-crystal data. Finally, the financial support from the State of Baden-Württemberg (Stuttgart, Germany) and the Open Access Publishing Fund of the University of Stuttgart is gratefully acknowledged.

Conflicts of Interest: The authors declare no conflict of interest.

References

1. Andac, O.; Glasser, F.P.; Howie, R.A. Dicalcium Sodium Fluoride Silicate. *Acta Crystallogr.* **1997**, *C 53*, 831–833. [[CrossRef](#)]
2. Hartenbach, I.; Schleid, Th. Na₃F[WO₄]: A Sodium Fluoride *Ortho*-Oxotungstate(VI) with Strands of Face-Shared Fluoride-Centred Sodium Octahedra According to {[FNa_{6/2}]²⁺}. *Z. Anorg. Allg. Chem.* **2007**, *633*, 524–526. [[CrossRef](#)]
3. Moutou, J.M.; Vlasse, M.; Cervera-Marzal, M.; Chaminade, J.P.; Pouchard, M.A. Structural Study of a New Lithium Oxyfluorotungstate, LiW₃O₉F. *J. Solid State Chem.* **1984**, *51*, 190–195. [[CrossRef](#)]
4. Abrahams, S.C.; Marsh, P.; Ravez, J. Structural Study of a New Lithium Oxyfluorotungstate, LiW₃O₉F. *Acta Crystallogr.* **1989**, *B 45*, 364–370. [[CrossRef](#)]
5. Hoard, J.L.; Vincent, W.B. Structures of Complex Fluorides. Potassium Hexafluogermanate and Ammonium Hexafluogermanate. *J. Am. Chem. Soc.* **1939**, *61*, 2849–2852. [[CrossRef](#)]
6. Srivastava, A.M.; Ackerman, J.F. Structure and Luminescence of Cs₂WO₂F₄: Efficient Luminescence of Isolated (WO₂F₄)²⁻ Octahedra. *J. Solid State Chem.* **1992**, *98*, 144–150. [[CrossRef](#)]
7. Udoenko, A.A.; Laptash, N.M. Disorder in Crystals of Dioxofluorotungstates, (NH₄)₂WO₂F₄ and Rb₂WO₂F₄. *Acta Crystallogr.* **2008**, *B 64*, 645–651. [[CrossRef](#)]
8. Mazej, Z.; Gilewski, T.; Goreshnik, E.A.; Jaglicic, Z.; Derzsi, M.; Grochala, W. Canted Antiferromagnetism in Two-Dimensional Silver(II) Bis[Pentafluorodioxidotungstate(VI)]. *Inorg. Chem.* **2017**, *56*, 224–233. [[CrossRef](#)]
9. Moutou, J.M.; Francisco, R.H.P.; Chaminade, J.P.; Pouchard, M.; Hagenmuller, P. Caracterisation Structurale de l'Oxyfluorotungstate de Cuivre CuWO₃F₂. *Z. Anorg. Allg. Chem.* **1986**, *539*, 165–174. [[CrossRef](#)]
10. Wingefeld, G.; Hoppe, R. Zur Konstitution von Ba₂WO₃F₄ und Ba₂MoO₃F₄. *Z. Anorg. Allg. Chem.* **1984**, *518*, 149–160. [[CrossRef](#)]
11. Torardi, C.C.; Brixner, L.H. Structure and Luminescence of Ba₂WO₃F₄. *Mater. Res. Bull.* **1984**, *20*, 137–145. [[CrossRef](#)]
12. Abrahams, S.C.; Marsh, P.; Ravez, J. Ferroelectric Structure and Related Properties of Pb₅W₃O₉F₁₀. *J. Chem. Phys.* **1987**, *87*, 6012–6020. [[CrossRef](#)]
13. Schleid, Th.; Strobel, S.; Dorhout, P.K.; Nockemann, P.; Binnemans, K.; Hartenbach, I. YF[MoO₄] and YCl[MoO₄]: Two Halide Derivatives of Yttrium *Ortho*-Oxomolybdate-Syntheses, Structures, and Luminescence Properties. *Inorg. Chem.* **2008**, *47*, 3728–3735. [[CrossRef](#)] [[PubMed](#)]
14. Schustereit, T.; Schleid, Th.; Hartenbach, I. Solvochemical Synthesis and Crystal Structure of the Fluoride-Derivatized Early Lanthanoid(III) *ortho*-Oxidomolybdates(VI) LnF[MoO₄] (Ln = Ce – Nd). *Eur. J. Inorg. Chem.* **2014**, *2014*, 5145–5151. [[CrossRef](#)]
15. Hartenbach, I.; Strobel, S.; Dorhout, P.K.; Schleid, Th. Crystal Structure, Spectroscopic Properties, and Magnetic Behaviour of the Fluoride-Derivatized Lanthanoid(III) *Ortho*-Oxomolybdates(VI) LnF[MoO₄] (Ln = Sm – Tm). *J. Solid State Chem.* **2008**, *181*, 2828–2836. [[CrossRef](#)]
16. Hartenbach, I.; Höpfe, H.A.; Kazmierczak, K.; Schleid, Th. Synthesis, Crystal Structure and Spectroscopic Properties of a Novel Yttrium(III) Fluoride Dimolybdate(VI): YFMo₂O₇. *Dalton Trans.* **2014**, *43*, 14016–14021. [[CrossRef](#)] [[PubMed](#)]

17. Müller, S.L.; Blaschkowski, B.; Hartenbach, I. No Pyroanions: The Representatives of the Lanthanoid(III) Fluoride Oxidodimolybdates(VI) $LnFMo_2O_7$ with the Smaller Cations ($Ln = Eu - Yb$). *J. Solid State Chem.* **2017**, *251*, 237–242. [[CrossRef](#)]
18. Rumble, J.R. (Ed.) *Handbook of Chemistry and Physics, Internet Version*, 98 ed.; CRC Press/Taylor & Francis: Boca Raton, FL, USA, 2019.
19. Perets, S.; Tseitlin, M.; Shneck, R.Z.; Mogilyanski, D.; Kimmel, G.; Burshtein, Z. Sodium Gadolinium Tungstate $NaGd(WO_4)_2$: Growth, Crystallography, and Some Physical Properties. *J. Cryst. Growth* **2007**, *305*, 257–264. [[CrossRef](#)]
20. Naruke, H.; Yamase, T. Structures of Novel $R_2Mo_5O_{18}$ and $R_6Mo_{12}O_{45}$ ($R = Eu$ and Gd) prepared by thermal decomposition of polyoxomolybdate precursor ($R_2(H_2O)_{12}Mo_8O_{27} \cdot nH_2O$). *Inorg. Chem.* **2002**, *41*, 6514–6520. [[CrossRef](#)]
21. Schustereit, T. Synthese und Charakterisierung anionischer Derivate von Seltenerdmetall-Oxidomolybdaten und -wolframaten mit Hilfe festkörper- und nasschemischer Methoden. Ph.D. Thesis, University of Stuttgart, Stuttgart, Germany, 2015.
22. Dorn, K.V. Synthese und Charakterisierung anionischer sowie lithiumhaltiger Derivate von Seltenerdmetall(III)-Oxidomolybdaten(VI) und -wolframaten(VI). Ph.D. Thesis, University of Stuttgart, Stuttgart, Germany, 2018.
23. Dorn, K.V.; Blaschkowski, B.; Förg, K.; Netzsch, P.; Höpfe, H.A.; Hartenbach, I. Prism Inside: Spectroscopic and Magnetic Properties of the Lanthanide(III) Chloride Oxidotungstates(VI) $Ln_3Cl_3[WO_6]$ ($Ln = La - Nd, Sm - Tb$). *Z. Anorg. Allg. Chem.* **2017**, *643*, 1642–1648. [[CrossRef](#)]
24. Hartenbach, I.; Strobel, S.; Schleid, Th.; Sarkar, B.; Kaim, W.; Nockemann, P.; Binnemans, K.; Dorhout, P.K. Synthesis, Structure, and Spectroscopic Properties of the New Lanthanum(III) Fluoride Oxomolybdate(VI) $La_3FMo_4O_{16}$. *Eur. J. Inorg. Chem.* **2010**, *2010*, 1626–1632. [[CrossRef](#)]
25. Sheldrick, G.M. *SADABS*; University of Göttingen: Göttingen, Germany, 1996.
26. Sheldrick, G.M. Crystal Structure Refinement with SHELXL. *Acta Crystallogr.* **2015**, *C 71*, 3–8.
27. Hahn, Th.; Wilson, A.J.C. *International Tables for Crystallography*, 2nd ed.; Kluwer Academic Publishers: Boston, MA, USA, 1992.
28. Fischer, R.X.; Tillmanns, E. The Equivalent Isotropic Displacement Factor. *Acta Crystallogr.* **1988**, *C 44*, 775–776. [[CrossRef](#)]
29. Hoppe, R. Madelung Constants as a new Guide in the Structural Chemistry of Solids. *Adv. Fluorine Chem.* **1970**, *6*, 387–438.
30. Hoppe, R. The Madelung Part of Lattice Energy, MAPLE, as a Guide in the Structural Solid State Chemistry. *Izv. Jugoslav. Centr. Krist. (Zagreb)* **1973**, *8*, 21–36.
31. Hoppe, R. The Madelung Part of Lattice Energy, MAPLE, as a Guide in Crystal Chemistry. In *Crystal Structure and Chemical Bonding in Inorganic Chemistry*; Rooymans, C.J.M., Rabenau, A., Eds.; North-Holland Publishers: Amsterdam, The Netherlands, 1975.
32. Hoppe, R. Effective Coordination Numbers (ECoN) and Mean Fictive Ionic Radii (MEFIR). *Z. Kristallogr.* **1979**, *150*, 23–52. [[CrossRef](#)]
33. Grzyb, T.; Wiglusz, R.J.; Nagirnyi, V.; Kotlov, A.; Lis, S. Revised crystal structure and luminescent properties of gadolinium oxyfluoride $Gd_4O_3F_6$ doped with Eu^{3+} ions. *Dalton Trans.* **2014**, *43*, 6925–6934. [[CrossRef](#)] [[PubMed](#)]
34. Brown, I.D.; Altermatt, D. Bond-Valence Parameters Obtained from a Systematic Analysis of the Inorganic Crystal Structure Database. *Acta Crystallogr.* **1985**, *B 41*, 244–247. [[CrossRef](#)]
35. Brese, N.E.; O'Keefe, M. Bond-Valence Parameters for Solids. *Acta Crystallogr.* **1991**, *B 47*, 192–197. [[CrossRef](#)]
36. Spirlet, M.-R.; Busing, W.R. Dodecatungstophosphoric acid-21-water by neutron diffraction. *Acta Crystallogr.* **1977**, *B 34*, 907–910. [[CrossRef](#)]
37. Lafuente, B.; Downs, R.T.; Yang, H.; Stone, N. The Power of Databases: The RRUFF Project. In *Highlights in Mineralogical Crystallography*; Armbruster, T., Danisi, R.M., Eds.; De Gruyter Publisher: Berlin, Germany, 2015; pp. 1–30.
38. Lin-Vien, D.; Colthup, N.B.; Fateley, W.G.; Grasselli, J.G. *Handbook of Infrared and Raman Characteristic Frequencies of Organic Molecules*; Academic Press: San Diego, CA, USA, 1991.
39. Socrates, G. *Infrared and Raman Characteristic Group Frequencies: Tables and Charts*, 3rd ed.; John Wiley & Sons: Chichester, UK, 2004.

40. Busca, G. Differentiation of Monooxo and Polyoxo and of Monomeric and Polymeric Vanadate, Molybdate and Tungstate Species in Metal Oxide Catalysts by IR and Raman Spectroscopy. *J. Raman Spectrosc.* **2002**, *33*, 348–358. [[CrossRef](#)]
41. Weidlein, J.; Müller, U.; Dehnicke, K. *Schwingungsfrequenzen I-Hauptgruppenelemente*, 1st ed.; Georg Thieme Verlag: Stuttgart, Germany, 1981.



© 2019 by the authors. Licensee MDPI, Basel, Switzerland. This article is an open access article distributed under the terms and conditions of the Creative Commons Attribution (CC BY) license (<http://creativecommons.org/licenses/by/4.0/>).